5. Schubauer, G. B., and H. K. Skramstad, *J. Res. Natl. Bur. Stand.*, **38**, 251 (1947).
6. Liepman, H. W., *Natl. Advisory Comm. Aeronaut. Rept. ACR No. 3H30* (August, 1943).
7. Klebanoff, P. S., G. B. Schubauer, and K. D. Tidstrom, *J. Aeronaut. Sci.*, **22**, 803 (1955).
8. Smith, A. M. O., and D. W. Clutter, *ibid.*, **26**, 229 (1959).
9. Tani, Itiro, and H. Komoda, *ibid.*, **29**, 440 (1962).
10. Adarkar, D. B., and W. M. Kays, *Stanford Univ. Dept. Mech. Eng. Tech. Rept. 55* (April 1, 1965).
11. Bryer, D. W., *Brit. Chem. Eng.*, **7**, 332 (1962).
12. Gould, R. W. F., *ibid.*, 667.
13. Taylor, G. I., *Phil. Trans. Royal Soc. (London)*, **A223**, 289 (1923).
14. Chandrasekhar, S., "Hydrodynamic and Hydromagnetic Stability," p. 272, Oxford Univ. Press, London (1961).
15. Bjorklund, I. S., and W. M. Kays, *J. Heat Transfer, Ser. C*, **81**, 175 (1959).
16. Ho, C. Y., J. L. Nardacci, and A. H. Nissan, *A.I.Ch.E. J.*, **10**, 194 (1964).
17. Biermann, David, and W. H. Herrnstein, *Natl. Advisory Comm. Aeronaut. Rept. 468* (1933).
18. Stuart, J. T., *Z. Angew. Math. Mech.*, **S-32**, 932 (1956).
19. Townsend, A. A., "Boundary Layer Research," H. Gortler, ed., p. 1, Springer-Verlag (1958).
20. Kestin, John, P. F. Maeder, and H. E. Wang, *Appl. Sci. Res.*, **A10**, 1 (1961).
21. Sherwood, T. K., and Olev Träss, *J. Heat Transfer*, **82C**, 313 (1960).
22. Eckert, E. R. G., and R. M. Drake, Jr., "Heat and Mass Transfer," 2 ed., McGraw-Hill, New York (1959).
23. Townsend, A. A., "Structure of Turbulent Shear Flow," Cambridge, p. 137, Univ. Press, London (1956).
24. Prandtl, Ludwig, "Essentials of Fluid Dynamics," p. 186, Blackie and Son, Ltd., London (1952).
25. Wille, R., in "Advances in Applied Mechanics," H. L. Dryden and Theodore von Karman, eds., Vol. 6, p. 280, Academic Press, New York (1960).

Manuscript received July 23, 1965; revision received September 27, 1965; paper accepted September 29, 1965.

Tracking Function Approach to Practical Stability and Ultimate Boundedness

W. O. PARADIS
University of Illinois, Urbana, Illinois
D. D. PERLMUTTER
University of Pennsylvania, Philadelphia, Pennsylvania

A graphical method of analysis is presented for studying the practical stability and ultimate boundedness of autonomous second-order systems. It is argued that these measures of stability are in many cases more germane to design than Liapunov stability. The method incorporates much of the geometric character of a Liapunov analysis, but it is shown that a Liapunov function, relatively difficult to obtain, can be replaced by a set of easily postulated scalar functions which collectively yield the required stability information. Examples are given which demonstrate the use and effectiveness of the method.

LaSalle and Lefschetz (7) have made a distinction between two kinds of stability that has important implications for engineering analysis. They consider *practical* stability as distinct from stability according to the definition of Liapunov. The distinction can be put in terms of mathematical δ, ϵ statements. For autonomous systems, Liapunov stability requires that there be a $\delta(\epsilon)$ for arbitrary $\epsilon > 0$, such that a trajectory starting in $||\mathbf{x}_0|| < \delta$ always be confined within $||\Phi|| < \epsilon$. In contradistinction practical stability requires only that *some* δ, ϵ combination exist of practical size; the quantities δ and ϵ correspond to regions in x space which are chosen a priori as the ranges of expected disturbances and allowable deviations, respectively. A necessary consequence of the definition is that the δ region be a subject of the ϵ region.

It is true that in many cases a system can be stable in both senses. On the other hand, one does not imply the other as can be seen from some simple counterexamples. Consider, for example, a phase-plane portrait such as Figure 1, which might represent the behavior of a stirred reactor similar perhaps to those studied by Aris and Amundson (*1*). A trajectory starting at A will move to

the (Liapunov) stable steady state B, but the system is not *practically* stable if the transient temperatures exceed the maximum allowable.

To show the opposite conclusion, consider (Figure 2) a system with limit cycle behavior like that in the study cited above or in the work of Gurel and Lapidus (*4*). The steady state here is unstable in the Liapunov sense, for there is no δ that satisfies the definition for an arbitrary choice of ϵ within the limit cycle. The system is, nevertheless, practically stable if the amplitudes of the limit cycle oscillations are within acceptable bounds. With the limit cycles shown in Figure 2, the system with first-order kinetics is practically stable, but the system with second-order kinetics is not if the ϵ region is identified with the limit cycle.

For engineering design, it is practical stability that is needed. It should be noted, however, that the design giving the largest region of proven stability is not necessarily the best, for it is performance quality that is important once stability has been assured. With regard to stability considerations, the problem is more properly one of establishing an acceptable δ, ϵ pair rather than one of attempting to insure stability under the widest possible range of conditions.

A system which is practically stable is, by definition, one in which the excursions of all state variables are confined to a fixed and acceptable range, the ϵ region. In certain cases, it may be possible to establish a region which, while bounding the transients, does not satisfy the size limitations of the prechosen ϵ region. In such a situation the notion of ultimate boundedness becomes useful (*5, 7*). A system is said to be ultimately bounded if there is a time $T > 0$ corresponding to each trajectory starting in $||\mathbf{x}_0|| < \delta$ such that $||\Phi|| < \lambda$ for all $t > T$. If practical stability cannot be assured it may suffice to bound the system behavior at sufficiently large times, that is, to determine a λ region such that λ is contained in ϵ.

In the discussion which follows, a method is presented for testing a class of systems for practical stability as well as ultimate boundedness. For clarity in presentation, the regions which result will be tacitly assumed to be of practical size and accordingly labeled as δ, ϵ, and λ. In practice, however, it would remain the task of the designer to check such regions against prechosen δ, ϵ, and λ regions as insurance that the results are indeed satisfactory.

TRACKING FUNCTIONS

One way to establish a region of asymptotic Liapunov stability which may also be a region of practical stability

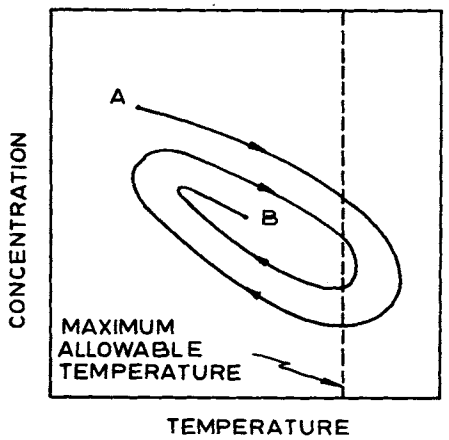

Fig. 1. Hypothetical system which is Liapunov stable but not practically stable.

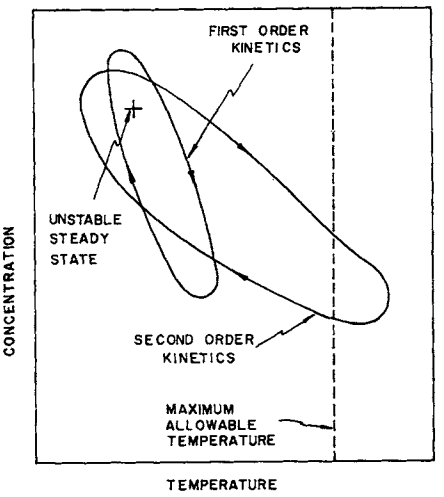

Fig. 2. System which is not Liapunov stable but may be practically stable.

is to find a Liapunov function $V(\mathbf{x})$ valid in a compact domain defined by $V(\mathbf{x}) \leq K$; that is

$$V(\mathbf{x}) = 0;\ \mathbf{x} = \mathbf{0}$$
$$V(\mathbf{x}) > 0;\ \mathbf{x} \neq \mathbf{0} \qquad (1)$$
$$\dot{V}(\mathbf{x}) \leq 0;\ \mathbf{x} \neq \mathbf{0}$$

However, in view of the foregoing considerations one might ask whether for autonomous systems practical stability could not be established by functions easier to find and to work with than those that meet the relatively stringent requirements of Equation (1). It will be shown in the following that such a region can be found for nonlinear systems of the form

$$\dot{x}_1 = f_1(x_1, x_2)$$
$$\dot{x}_2 = f_2(x_1, x_2) \qquad (2)$$

by choosing sets of simple tracking functions $E_i(\mathbf{x})$ such that a closed broken curve is formed by a succession of contours $E_i(\mathbf{x}) = K_i$. This procedure has some similarity to the AERP (alternate extreme radius path) approach of Leathrum, Johnson, and Lapidus (*8*) but, as will be shown, the detailed arguments are essentially different.

Consider a phase plane as in Figure 3 to be divided into n regions by a series of lines along which $\dot{E}_i = 0$. Accordingly, $\dot{E}_i$ is of fixed sign in the i^{th} region adjacent to the line, and the path of any trajectory in the i^{th} region can be restricted as to whether it crosses $E_i = K_i$ contours in the direction of increasing or decreasing K_i. Suppose for definiteness that each $\dot{E}_i < 0$ and that each $a_{i_1} > a_{i_2} > a_{i_3}$. Further assume that a trajectory starting from a point on HA must move to the right. The broken line $ABCDFGHA$ serves as a boundary on both the δ and ϵ regions. The enclosed area is a region of practical stability, since any trajectory within this boundary is for all time confined within it (the corresponding E must decrease along the trajectory). The argument remains essentially unchanged if the inequality directions are reversed on any $\dot{E}_i$ and a_i set. Although it is not required for the argument, it is convenient to choose the $E_i(\mathbf{x})$ functions so that

$$E_i = 0;\ \mathbf{x} = \mathbf{0} \qquad (3)$$

and to avoid an $E(\mathbf{x})$ that gives

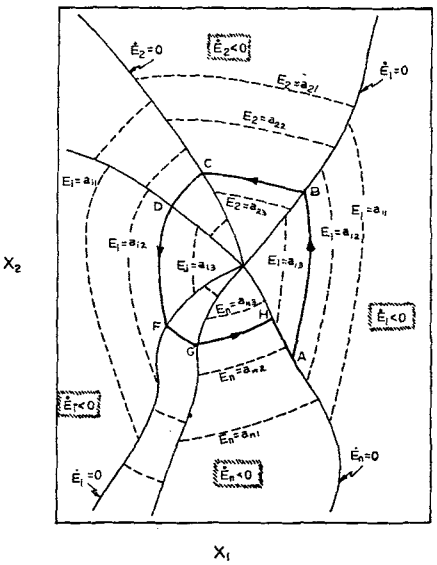

Fig. 3. Tracking function analysis in the phase plane.

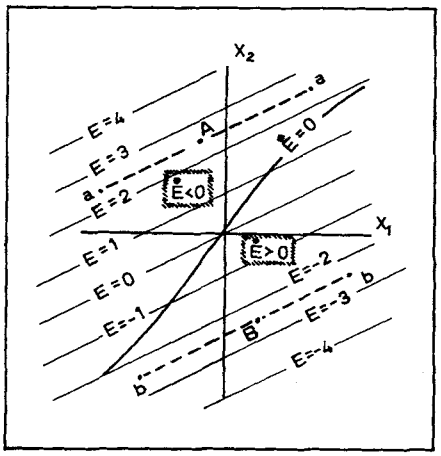

Fig. 4. Graphical representation of $E = -mX_1 + X_2$ for a particular choice of the constant m.

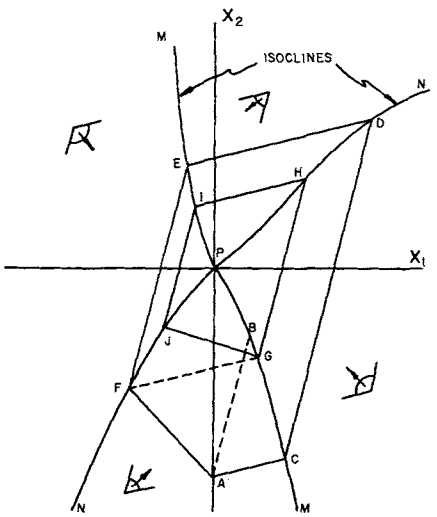

Fig. 5. Use of isoclines to fix a region of stability.

$$\dot{E}_i = E_i = 0 \tag{4}$$

at more than a finite number of isolated points.

Obviously, a wide class of functions satisfies these conditions. Very satisfactory results can usually be obtained, however, from the simplest choices, straight lines and circles:

$$E = -m\ x_1 + x_2 \tag{5}$$

$$E = (x_1 - \alpha_1)^2 + (x_2 - \alpha_2)^2 \tag{6}$$

To see that this is the case, consider Equation (5). By differentiation

$$\dot{E} = -m\ \dot{x}_1 + \dot{x}_2 \tag{7}$$

For a particular choice of m, the contours of constant E and the locus of $\dot{E} = 0$ might be represented as in Figure 4. Within the confines of the plot, a solution path through point A cannot pass above the line aa (E must decrease with time), while one through B cannot pass below the line bb (E must decrease with time). The $\dot{E} = 0$ locus is, of course, merely a selected isocline in this case. Such isoclines are customarily used to provide a rough estimate of the solution behavior. They also divide the plane into regions for which definite bounds on the trajectory path may be associated.

In Figure 5 two isoclines divide the plane into four regions. Within each region trajectories are restricted to a motion within the respective E contour, as indicated by the symbol in that region. The direction of motion is easily obtained by evaluating $\dot{x}_i$ ($= dx_i/dt$) or $\dot{x}_2$ at any point in the plane other than the origin. For example, a trajectory passing through point A must eventually cross the MM line along the segment BC. From the segment BC, the trajectory must successively cross the isoclines along the segments DP, EP, FP, and so on to JP. Although the exact path of the trajectory is unknown, it is confined within $ACDEFA$.

It is evident that from any initial conditions within the region $ACDEFA$, the trajectory must converge at least to the region $GHIJG$. The possibility of a limit cycle within $GHIJG$ cannot be excluded, but continuing the graphical construction further reduces the size of the possible limit cycle so long as convergence of the limiting path is obtained. As constructed, the region $ACDEFA$ would correspond to both a δ region and an ϵ region, and thus define a region of practical stability. Moreover, $GHIJG$ serves as a λ region into which the trajectory must pass and remain at sufficiently large time.

The potential usefulness of isoclines in a stability analysis is thus apparent, but since the method can be applied to $E(\mathbf{x})$ functions other than Equation (5), it is not limited to a study of isoclines. The $\dot{E} = 0$ locus for the circular $E(\mathbf{x})$ of Equation (6) is, for example, *not* an isocline; still it can be used as described above to limit possible trajectories. Furthermore, in some cases regions can be established from within which trajectories must ultimately emerge. By using this argument, it is possible for us to prove that limit cycles exist in some systems.

In effect, a single Liapunov function with very powerful properties is discarded in favor of several functions, each less powerful than the original, which yield collectively the desired stability information. The salient feature of the approach is that the required functions may be easily postulated and used. Moreover, although the results will always be conservative (sufficient but not necessary), a means of obtaining less conservative results is available. Thus the method serves to utilize the geometrical arguments of a Liapunov analysis in a way which can readily be applied in practice.

In the last analysis, the usefulness of the method depends upon being able to fix regions of practical stability

with a reasonably small set of E functions. With this in mind, three well-known systems are analyzed below. Where possible, he results are compared with those obtained by other means.

VAN DER POL EQUATION

The equation of Van der Pol may be written as

$$\frac{d^2y}{dt^2} - e\,(1-y^2)\,\frac{dy}{dt} + ay = 0;\ e, a > 0 \qquad (8)$$

where e and a represent constants here taken as 0.1 and 1.0 respectively. Letting $x_1 = y$ and $x_2 = dy/dt$, we can express Equation (8) in the form of Equation (2):

$$dx_1/dt = x_2$$
$$dx_2/dt = 0.1\,(1-x_1^2)\,x_2 - x_1 \qquad (9)$$

with a singular point at the origin.

The loci plotted in Figure 6 satisfy the algebraic equations $\dot{E}_i = 0$, $i = 1, 2, 3, 4, 5$, where

$$\begin{aligned} E_1 &= x_1 \\ E_2 &= x_2 \\ E_3 &= x_1 + x_2 \\ E_4 &= x_1 - x_2 \\ E_5 &= x_1^2 + x_2^2 \end{aligned} \qquad (10)$$

Each of the first four of these loci is an isocline which, in effect, bounds the solution path to a known 45 deg. angle in the x_1, x_2 plane. The $\dot{E}_5 = 0$ loci provide additional information. Within the strip $x_2 = \pm 1$, it is easily shown that $\dot{E}_5 > 0$. From any point within this strip, the solution path must therefore encounter circles (about the origin) of increasing radius for as long as the motion remains within the strip. Outside the strip $\dot{E}_5 < 0$, and the motion must tend toward the origin passing through circles of smaller radius.

For clarity, the loci are reconstructed as dotted lines in Figure 7. A point on the plane is selected and the most divergent path consistent with known information is pursued. As regards Figure 7, the trajectory begins at the arbitrarily selected point labeled A. At point A it is known that: the angle of departure θ must be such that $0 \leq \theta \leq 45$ deg., and the limiting path must be moving away from the origin. Accordingly, the path is that which intersects the $\dot{E}_2 = 0$ locus along a 45 deg. line from A. This establishes point B. From point B, the most divergent path is a horizontal line to point C. Similarly, the entire limiting path is easily plotted step-by-step, that is

From	To	Limiting path is:	Described by:
C	D	arc of circle about origin	E_5 = constant
D	E	−45 deg. line	E_3 = constant
E	F	arc of circle about origin	E_5 = constant
. . . . .			
V	W	−135 deg. line	E_4 = constant

In this manner the closed curve $WHI \ldots UVW$ is finally obtained. The curve acts to bound both the δ region and the ϵ region required for practical stability. Any trajectory originating within this closed curve must remain within its confines for all time. It can be further shown that trajectories originating outside the curve must eventually cross into the closed region remaining there everafter. Thus in terms of ultimate boundedness the entire phase plane becomes the δ region, the curve $WHI \ldots UVW$ then corresponding to the λ region. It was noted above that from any point within a circle of unit radius, trajectories must diverge at least to the unit circle. Then since no other critical points exist besides the origin, a limit cycle must exist as a closed curve about the origin within the annular area. As will be demonstrated in the next example, the size of the area of uncertainty, in this case the annular area, may be reduced by the use of new information gained by considering additional tracking functions.

For comparison, other treatments of this problem include a study of the linearized equations, application of Liapunov's direct method, and numerical solutions for selected initial conditions. Taking these in order, we see that the characteristic roots of the linearized equations indicate a single unstable critical point at the origin. (the origin is either an unstable node or an unstable focus according to the value of e). No hint as to the existence of a limit cycle can be obtained by this approach and the technique is totally unable to locate regions of stability.

Liapunov's direct method has been applied to this particular problem with considerable success (7). From Equation (8), the analysis makes use of the transformation $z_1 = y$, $\dot{z}_2 = -y$ to obtain the set of equivalent equations

$$dz_1/dt = z_2 - e\,(z_1^3/3 - z_1) \qquad (11)$$
$$dz_2/dt = -z_1$$

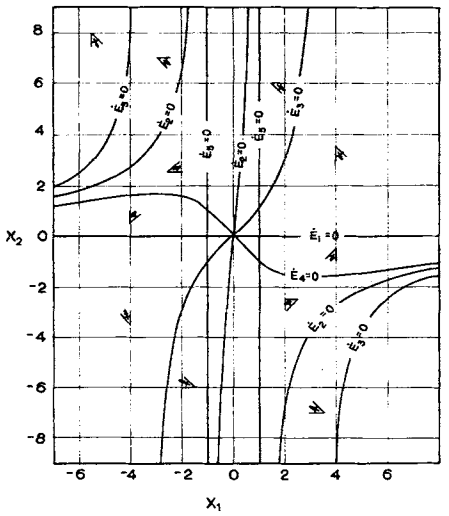

Fig. 6. Loci for $\dot{E}_i = 0$, $i = 1,2,3,4,5$ for the Van der Pol equation.

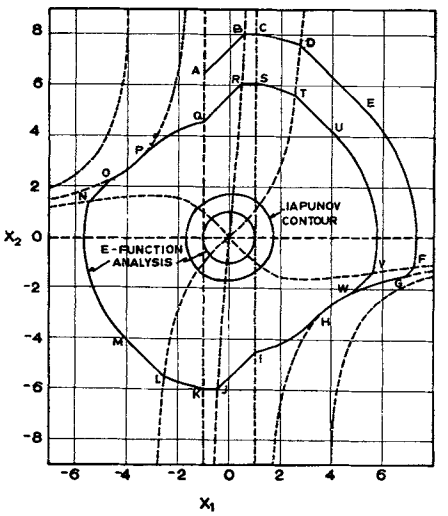

Fig. 7. Stability analysis of the Van der Pol equation.

A Liapunov function is taken as

$$V(z_1, z_2) = (z_1^2 + z_2^2)/2 \qquad (12)$$

from which it can be shown that if a limit cycle exists, it must be exterior to a circle of radius $\sqrt{3}$ in the z_1, z_2 plane. By transforming coordinates, we see that the circle is given by the locus of all points satisfying the equation

$$x_2 = \frac{e}{3} x_1 (3 - x_1^2) \pm (3 - x_1^2)^{1/2} \qquad (13)$$

in the x_1, x_2 plane. This curve is shown in Figure 7 for comparison with those obtained by the E function technique.

The Liapunov contour and the unit circle of the E function method correspond in that they each enclose a region of instability, that is, from within, all solution paths must leave either region as $t \to \infty$. On this point, the Liapunov approach is superior, since a larger region of instability is demonstrated; however, the remaining conclusions drawn from the E function analysis are unattainable by the Liapunov analysis. It may be noted that the Liapunov function of Equation (12) satisfies completely the requirements of an E function, as do, in fact, all acceptable Liapunov functions [Equation (1)]. Consequently, all information gained by the Liapunov analysis could, in principal, be obtained by the E function approach.

The most complete description of the system is obtained by numerically solving the Van der Pol equation repeatedly for various initial conditions. In this manner the transient performance, as well as the stability of the system, may be characterized. Solutions for the parameter values considered here are given in the literature (3). The results indicate that all trajectories converge in a clockwise fashion onto a limit cycle nearly circular of radius two. It should be noted that solution of the differential equations normally yields more complete results at the cost of increased computation time.

MULTIPLE SINGULAR POINTS

Because of the importance of multiple steady states in chemical reactor systems (1, 6), it is interesting to test the tracking function approach on an example with two singular points, suggested by LaSalle and Lefschetz (7). Consider a dynamic system represented by the equation

$$\ddot{y} + 2\dot{y} + 6y + 3y^2 = 0 \qquad (14)$$

or its equivalent

$$\dot{x}_1 = x_2$$
$$\dot{x}_2 = -6x_1 - 2x_2 - 3x_1^2 \qquad (15)$$

where $x_1 = y$, $x_2 = \dot{y}$. Singular points of Equation (15) are at the origin (0, 0) and at (−2, 0).

The following initial set of E functions is chosen:

$$\begin{aligned} E_1 &= x_1 \\ E_2 &= x_2 \\ E_3 &= x_1 + x_2 \\ E_4 &= x_1 - x_2 \\ E_5 &= x_1^2 + x_2^2 \\ E &= (x_1 + 2)^2 + x_2^2 \end{aligned} \qquad (16)$$

As in the first example, a plot of the $\dot{E}_4 = 0$ loci serves as a basis for the stability analysis. The results are shown in Figure 8. Curve A encloses a δ, ϵ region of practical stability in that all trajectories originating within A must remain within A for all time. The curve itself is a piecewise connected series of constant E_4 loci, each function being a member of Equation (16). In a manner similar to that used in obtaining the λ region of Figure 5, it can

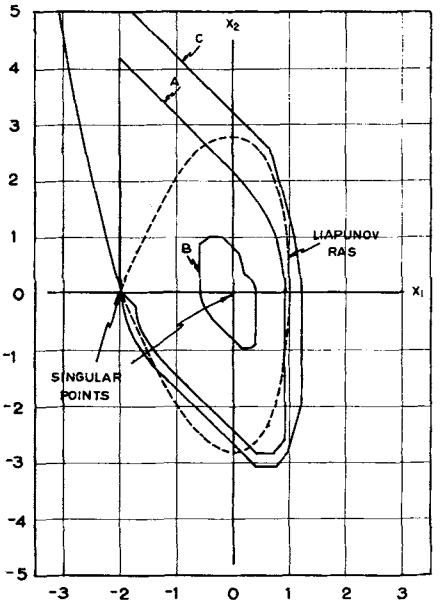

Fig. 8. Results of stability analysis for system with two singular points.

be shown that all trajectories originating in the δ region, that is, within A, will be ultimately bounded by a λ region interior to the closed curve B.

If it is desired to either increase the size of the δ, ϵ region or decrease that of the λ region, further tracking functions are required. Suppose two additional functions are chosen as

$$E_7 = x_1 + 0.25\,x_2$$
$$E_8 = x_1 - 0.25\,x_2$$

With little extra effort, the analysis now leads to improved results. Bounded by curve C, the δ, ϵ region has been enlarged somewhat and, perhaps more important, the λ region has become so small that, to the limits of graphical accuracy, it contains only the singular point (0, 0). Thus, from anywhere within C, solutions are forever confined to that region and must eventually approach and remain within a tiny λ region about the singular point at the origin. For design purposes, the δ region defines a region of asymptotic stability as well as practical stability.

A Liapunov analysis of Equation (15) (7) indicates a region of asymptotic stability for the closed region bounded by the locus of points satisfying the equation

$$x_2^2/2 + 3x_1^2 + x_1^3 = 4 \qquad (18)$$

This region is plotted for comparison.

In the first two examples, the δ region of expected disturbances and the ϵ region of allowable or resulting deviations were, in fact, one and the same region. As will be shown below the two regions often coincide by choice, not by necessity.

ANALYSIS OF A CHEMICAL PROCESS

Turning to a somewhat more practical example, consider a well stirred reactor which can be described by an energy balance and a material balance:

$$\rho V C_p \frac{dT}{dt} = \Delta H V r - UA_r (T - T_a) - \rho q C_p (T - T_o)$$
$$V \frac{dc}{dt} = -Vr - q(c - c_o) \qquad (19)$$

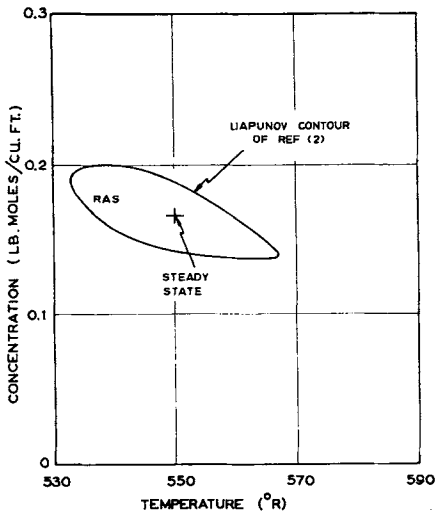

Fig. 9. Liapunov analysis of a stirred tank reactor.

Using the notation of reference 2, also defined in the notation, we reduce Equation (19) to

$$\frac{d\hat{\eta}}{dt} = \frac{\hat{r}}{c_o} - \frac{b}{a}\hat{\eta}$$

$$\frac{d\hat{y}}{dt} = \frac{-\hat{r}}{c_o} - \frac{1}{\tau}\hat{y} \qquad (20)$$

with the steady state solution at the origin, $\hat{\eta} = \hat{y} = 0$. A stability analysis (2) using Liapunov's direct method established a region of asymptotic stability (RAS) shown in Figure 9 for a first-order reaction rate of the form $r = cA \exp(-Q/T)$ and the selected parameter values:

$A = 10^8$ hr.$^{-1}$
$Q = 10^4$ °R.
$U = 5$ B.t.u./(hr.)(sq. ft.)(°F.)
$A_r = 100$ sq. ft.
$V = 100$ cu. ft.
$c_o = 0.270$ lb.-mole/cu. ft.

$C_p = 1.0$ B.t.u./(lb.)(°F.)
$\rho = 50$ lb./cu. ft.
$T_o = T_a = 530$°R.
$\Delta H = 10^4$ B.t.u./lb.-mole
$q = 200$ cu. ft./hr.

For comparisons a simple set of E functions may be chosen as

$$E_1 = \hat{\eta}$$
$$E_2 = \hat{y}$$
$$E_3 = \hat{\eta} + \hat{y} \qquad (21)$$
$$E_4 = \hat{\eta} - \hat{y}$$

The corresponding time derivatives are given by the equations

$$\dot{E}_1 = \frac{\hat{r}}{c_o} - \frac{b}{a}\hat{\eta}$$

$$\dot{E}_2 = \frac{-\hat{r}}{c_o} - \frac{1}{\tau}\hat{y}$$

$$\dot{E}_3 = \frac{-b}{a}\hat{\eta} - \frac{1}{\tau}\hat{y} \qquad (22)$$

$$\dot{E}_4 = \frac{2\hat{r}}{c_o} - \frac{b}{a}\hat{\eta} + \frac{1}{\tau}\hat{y}$$

For the given parameter values, the loci satisfying $\dot{E}_i = 0$, $i = 1, 2, 3, 4$ are plotted in Figure 10. Point A is arbitrarily selected as a starting point, and the limiting path is pursued. As shown, convergence is obtained to as close to the origin as graphical accuracy permits. By selecting another point, say point B, we reach the same conclusion. Two regions of practical stability are immediately obtained by connecting the ends of the limiting paths with straight lines OA and OB.

Other regions of practical stability are also readily available. Suppose, for example, the δ region of expected disturbances is taken as the circular area enclosed by the curve $\hat{\eta}^2 + (4\hat{y})^2 = 0.16$. The corresponding ϵ region is found by following the circular path and leaving that path to pursue a more divergent path whenever possible. The dotted line in Figure 10 represents the resulting curve which encloses the ϵ region. The two regions do not, however, coincide. The δ region of initial disturbances need not be restricted to a particular size or shape; it should correspond to the closed region about the steady state within which the initial conditions, or equivalent impulse perturbations, are expected to lie.

A second facet of the analysis, quite distinct from practical stability, concerns finding the largest possible region for which asymptotic stability can be assured. Again referring to Figure 10, it is evident that solutions from any point to the left of the broken line DEF must converge to the origin. This clearly encompasses a much larger region than that obtained by the Liapunov analysis (see Figure 9). The size of the tracking function RAS is limited

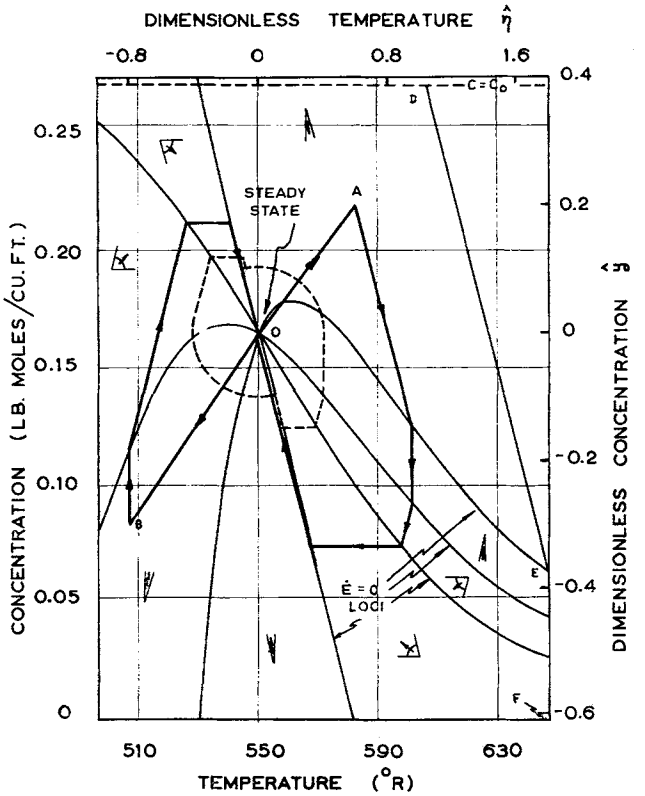

Fig. 10. Tracking function analysis of a stirred tank reactor.

in this example only by the η scaling on the graph itself. With the given set of tracking functions, it is, in fact, possible to demonstrate asymptotic stability for a region of arbitrary size.

DISCUSSION

By using a set of tracking functions, the analyst may extract from the system equations enough information to outline regions of practical stability and ultimate boundedness. In many cases, however, the design specifications may not allow a definite preconceived notion as to the desired δ, ϵ, and λ regions. The problem may be to discover the control mode or variable parameter settings which provide the largest δ region for a given ϵ region, or the smallest ϵ region for a given δ region. Or, it may be desired to ultimately bound trajectories from a given δ region by the smallest possible λ region, or find the largest δ region for a given λ region. In any case the problem is, from an engineering standpoint, something more than simply being able to demonstrate the largest possible RAS. It is in this light that the use of tracking functions provides an especially effective approach to the problem.

This technique may be compared to the available alternatives. It has the important advantage of Liapunov analysis: the conclusions are valid for regions rather than points on the phase plane. The results are always conservative (sufficient, not necessary), but in contrast to the direct method, the tracking function analysis lends itself well to successive approximations. New information from additional E functions may always be superimposed on earlier results to enlarge or reduce regions of interest. The method is simple, the greatest share of the work being spent on determining the $\dot{E} = 0$ loci. In the examples considered, the computations were less involved than those of the corresponding Liapunov analyses. In comparison to a numerical integration of the phase plane equation, there are two immediate advantages in solving for the $\dot{E} = 0$ loci. Far fewer solution points are normally required since the calculations need not be repeated for various initial conditions. Moreover, the equations are algebraic rather than differential. Consequently, there is no chance for cumulative error, and the computation intervals may be greatly enlarged.

On the other hand, there is no guarantee that a given set of E functions will yield the necessary stability information. In certain cases so many functions might be needed as to make the method impractical. For the examples considered, this number was seen to be reasonably small. Similarly, a Liapunov analysis ceases to be practical when a suitable Liapunov function is unavailable.

As noted above, another stability criterion applicable to systems taking the form of Equation (2) recently has been developed by Leathrum, Johnson, and Lapidus. In certain respects their method resembles the E function approach: an alternating extreme radius path (AERP) is defined which, when graphically constructed, either converges, closes upon itself, or diverges with respect to an equilibrium point of the system equations. Examples are given (8) which demonstrate that the stability of the AERP is related to the stability of the actual system, although no general proof of such a relationship presently exists.

The distinction between the AERP method and that of E functions is a basic one. The AERP is in a sense an *estimate* of the solution path, while E functions are used to obtain a *bound* on the solution path. It is impossible to obtain an AERP from the concept of limiting paths and, in fact, the two are essentially independent. While an AERP analysis determines the behavior of the system as $t \to \infty$, it does not attempt to bound the behavior of the system during the transient period. On the other hand, the tracking function approach inherently provides limits on the phase plane solution path throughout the transient period. For this reason the important question of practical stability (which depends on the transient behavior) seems more suitably attacked by an E function type of approach. With regard to the behavior of the system at $t \to \infty$, the two methods yield similar results by different means.

ACKNOWLEDGMENT

The support of this research by the National Science Foundation is gratefully acknowledged.

NOTATION

A = frequency factor
A_r = reactor area
a = $\rho V c_p$
b = $UAr + \rho q c_p$
C_p = specific heat
c = concentration
E = scalar tracking function
ΔH = heat of reaction
Q = activation energy divided by the gas constant
q = volumetric flow rate
r = rate of reaction per unit volume = $Ace^{-Q/T}$
T = temperature
t = time
U = overall heat transfer coefficient
V = reactor volume
$\mathcal{V}$ = Liapunov function
$\mathbf{x}$ = general state vector
y = normalized concentration = c/c_o
δ = region of initial conditions
ϵ = region of allowable deviations

Greek Letters

η = normalized temperature = $\rho c_p T/\Delta H c_o$
λ = region of ultimate boundedness
Φ = a solution of Equation (2)
ρ = density
τ = time constant = V/q
θ = angle

Subscripts and Superscripts

$\wedge$ = deviation from steady state
$\cdot$ = total time derivative
$\| \ \|$ = norm of a vector
o = input and initial condition
a = ambient

LITERATURE CITED

1. Aris, Rutherford, and N. R. Amundson, *Chem. Eng. Sci.*, **7**, 121 (1958).
2. Berger, J. S., and D. D. Perlmutter, *A.I.Ch.E. J.*, **10**, 233, 238 (1964).
3. Davis, H. T., "Introduction to Nonlinear Differential and Integral Equations," U. S. Atomic Energy Commission (1960).
4. Gurel, Okan, and Leon Lapidus, *Chem. Eng. Progr. Symposium Ser. No. 55*, **61**, 78-87 (1965).
5. Hahn, Wolfgang, "Theory and Application of Liapunov's Direct Method," Prentice Hall, Englewood, N. J. (1963).
6. Hoftyzer, P. J., and T. N. Zwietering, *Chem. Eng. Sci.*, **14**, 241 (1961).
7. LaSalle, Joseph, and Solomon Lefschetz, "Stability by Liapunov's Direct Method," Academic Press, New York (1961).
8. Leathrum, J. F., E. F. Johnson, and Leon Lapidus, *A.I.Ch.E. J.*, **10**, 16 (1964).

Manuscript received May 26, 1965; revision received September 16, 1965; paper accepted September 17, 1965. Paper presented at A.I.Ch.E. Philadelphia meeting.